

# Evaluation of Inner Retinal Layers in Eyes With Temporal Hemianopic Visual Loss From Chiasmal Compression Using Optical Coherence Tomography

Mário L. R. Monteiro,<sup>1</sup> Kenzo Hokazono,<sup>1</sup> Danilo B. Fernandes,<sup>1</sup> Luciana V. F. Costa-Cunha,<sup>1</sup> Rafael M. Sousa,<sup>1</sup> Ali S. Raza,<sup>2,3</sup> Diane L. Wang,<sup>2</sup> and Donald C. Hood<sup>2,4</sup>

<sup>1</sup>Division of Ophthalmology, University of São Paulo Medical School, São Paulo, Brazil

<sup>2</sup>Department of Psychology, Columbia University, New York, New York, United States

<sup>3</sup>Department of Neurobiology and Behavior, Columbia University, New York, New York, United States

<sup>4</sup>Department of Ophthalmology, Columbia University, New York, New York, United States

Correspondence: Mário L. R. Monteiro, Av. Angélica 1757 conj. 61, 01227-200, São Paulo, SP, Brazil; mlrmonteiro@terra.com.br.

Submitted: February 7, 2014

Accepted: April 9, 2014

Citation: Monteiro MLR, Hokazono K, Fernandes DB, et al. Evaluation of inner retinal layers in eyes with temporal hemianopic visual loss from chiasmal compression using optical coherence tomography. *Invest Ophthalmol Vis Sci.* 2014;55:3328–3336. DOI:10.1167/iovs.14-14118

**PURPOSE.** We measured macular inner retinal layer thicknesses using frequency-domain optical coherence tomography (fd-OCT) and correlated these measures with visual field (VF) in eyes with temporal hemianopia from chiasmal compression and band atrophy (BA) of the optic nerve.

**METHODS.** Macular fd-OCT scans and VFs were obtained from 33 eyes of 33 patients with temporal hemianopia and 36 control eyes. The macular retinal nerve fiber layer (mRNFL), combined retinal ganglion cell and inner plexiform layers (RGCL+), and the inner nuclear layer (INL) were segmented. Measurements were averaged for each macula quadrant. Scans were assessed qualitatively for microcysts in the INL. The VF was estimated from the central 16 test points. The two groups were compared. Correlations between VF and OCT measurements were assessed.

**RESULTS.** The mRNFL, RGCL+, and total retinal (TR) macular thickness measurements were significantly smaller in BA eyes than controls. In the nasal quadrants, INL measurements were significantly greater in BA eyes than controls. The mRNFL and RGCL+ measurements had greater discrimination ability than TR measurements in the temporal quadrants. A significant correlation was found between most OCT parameters and their corresponding VF parameters. The strongest association was observed between RNFL and RGCL+ thickness, and VF loss in the corresponding area. The INL microcysts were found in seven eyes with BA, but not in controls.

**CONCLUSIONS.** Band atrophy leads to mRNFL and RGCL+ thinning, and INL thickening, and mRNFL and RGCL+ measurements are correlated strongly with VF loss. Segmented macular thickness measurements may be useful for quantifying neuronal loss in chiasmal compression.

**Keywords:** optical coherence tomography, retinal ganglion cell layer thickness, retinal nerve fiber layer, inner nuclear layer, macular thickness, band atrophy

Clinical evaluation and management of anterior visual pathway diseases is dependent largely on functional visual testing, and morphologic assessment of the optic nerve, peripapillary retinal nerve fiber layer (RNFL), and retinal ganglion cells (RGCs). In the past decade, optical coherence tomography (OCT) was introduced as a means of detecting retinal abnormalities, including those resulting from axonal loss in diseases, such as glaucoma and hereditary, demyelinating, or compressive lesions of the anterior optic pathways.<sup>1–4</sup> Patients with chiasmal lesions provide an interesting model for assessing the ability of new technologies to quantify axonal loss, and for investigating the relationship between functional and structural measurements. In patients with midchiasmal lesions, temporal hemianopia, and preserved nasal field, the crossed nerve fibers are lost with preservation of the uncrossed nerve fibers, which originate in the temporal hemiretinal, and penetrate the optic nerve through the superior and inferior arcuate fiber bundles. Thus, RNFL loss occurs predominantly on the nasal and

temporal side of the optic disc, a pattern identified on ophthalmoscopy as band atrophy (BA) of the optic nerve,<sup>5</sup> and the retina shows a clear distinction in axonal loss when the temporal hemiretina is compared to the affected nasal hemiretina.

Previous studies have demonstrated that OCT-measured retinal thickness measurements can detect neural loss in patients with chiasmal compression, and that such measurements are able to identify the pattern of axonal loss found in this condition, based on OCT measurements of the peripapillary RNFL and macular full-thickness measurements.<sup>6–8</sup> While such studies indicate that visual function correlates significantly with peripapillary RNFL thickness and macular thickness, the former generally is equivalent or outperforms the latter in terms of magnitude of association with visual function.<sup>8–10</sup> This may be explained by the fact that macular thickness is a less specific measure (equivalent to total retinal thickness) and includes structures other than the RGC layer (RGCL).

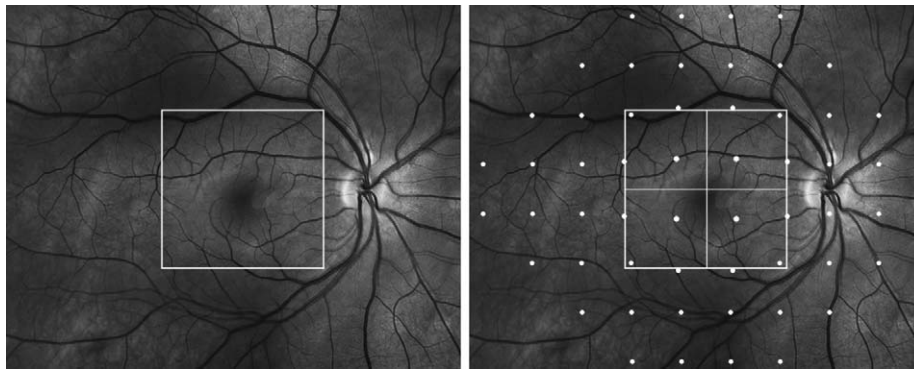


**FIGURE 1.** *Left:* Demarcation of area in the macula scanned by fd-OCT. *Right:* Demarcation of points read on 24-2 standard automated perimetry. The 16 points, positioned to account for the displacement of the retinal ganglion cell bodies as suggested previously in the literature,<sup>40</sup> roughly correspond to the central square area covered by fd-OCT scanning.

Today, neural loss may be evaluated by measuring specific groups of cells (such as RGCs) affected in different disorders of the anterior optic pathway. Recent studies based on segmented OCT macular thickness measurements have demonstrated that the presence of RGC loss may be an early indicator of neural loss in conditions, such as glaucoma, multiple sclerosis (MS), and neuromyelitis optica (NMO).<sup>11-15</sup> The widespread use of frequency-domain OCT (fd-OCT) also has generated a large body of data regarding structural abnormalities in the retina, not only in the RNFL and RGCL (which are expected to be affected), but also in the inner nuclear layer (INL), including microcystic degeneration of the INL in patients with MS, NMO, and glaucoma.<sup>16-21</sup> Although INL microcysts have been reported in patients with chiasmal glioma,<sup>22</sup> to our knowledge no previous study has used OCT systematically to evaluate the thickness of different macular layers and structural abnormalities in patients with chiasmal compression from pituitary adenomas.

The purpose of this study, therefore, was to evaluate the thickness of the inner retinal layers in patients with BA of the optic nerve using fd-OCT and a computer-aided manual segmentation procedure. The ability of this technique to discriminate normal eyes from eyes with BA of the optic nerve was evaluated, and compared to conventional peripapillary RNFL and macular full-thickness measurements. The relation between functional damage and structural damage of the macula also was considered. Finally, we examined the sample for structural abnormalities, including microcysts in the INL.

## METHODS

### Subjects

This was an observational, prospective cross-sectional study. A total of 33 patients (20 male, 13 female) with temporal hemianopia from chiasmal compression and 36 controls (14 male, 22 female) were recruited for examination at the Division of Ophthalmology of the University of São Paulo Medical School. All patients had been submitted to previous treatment of the suprasellar lesion and had stable visual field (VF) defects for at least 1 year before study entry. Twenty-nine patients had pituitary adenoma, three had craniopharyngioma and one had suprasellar meningioma. Approval from the Institutional Review Board Ethics Committee was obtained for the study. The study followed the principles of the Declaration of Helsinki and informed consent was obtained from all participants.

The inclusion criteria for the study were best-corrected visual acuity of 20/30 or better in the study eye, spherical refraction within  $\pm 5$  diopters for the most ametropic meridian, IOP < 22 mm Hg, and reliable VF. Patients with a history of intraocular diseases, or with clinical signs of glaucoma or other optic disc anomalies were excluded.

Patients with BA were required to have complete or partial temporal hemianopia and a nasal hemifield within normal limits on standard automated perimetry (SAP). The minimum criteria for defining a VF as abnormal was the presence of at least two nonedge-contiguous test points, not including those directly above and below the blind spot, with a pattern deviation (PD plot) of one point with  $P < 0.5\%$  and one point with  $P < 2\%$ . A normal nasal hemifield was defined as the absence of any cluster of at least 3 points with  $P < 5\%$  on the PD plot. Only one eye of each patient was selected for analysis. In 26 patients, only one of the eyes met the inclusion criteria. In the seven patients in whom both eyes fulfilled the inclusion criteria, one eye was selected randomly for analysis. The control group consisted of normal healthy volunteers recruited from among the hospital staff. All normal subjects had normal ophthalmic findings and normal VF. A normal VF was defined as a pattern standard deviation (PSD) within the 95% confidence limits and a Glaucoma Hemifield test result within normal limits. One eye of each healthy subject was included for analysis.

### OCT and Segmentation Technique

Subjects underwent fd-OCT scanning of the macular area without dilating the pupil, using commercially available equipment (3D OCT-1000; Topcon Corp., Tokyo, Japan) on the same day of the ophthalmic evaluation. The authors reviewed the images with respect to their subjective and objective quality.

The scanning protocol involved the acquisition of a set of three high-definition OCT images of the macula in a raster pattern covering a 6-mm area (Fig. 1) with a scan density of  $512 \times 128$  in approximately 3.5 seconds (27,000 A-scans/s). Criteria for acceptable images included an absence of large eye movements, defined as an abrupt shift completely disconnecting a large retinal vessel; a consistent signal intensity level across the scan; and an absence of black bands (caused by blinking) throughout the scan.

Local structural thickness was determined for the individual B-scans of the cube scan. In each B-scan, the boundaries between the anatomical layers were determined using a previously validated automated segmentation algorithm,<sup>23</sup> which then was hand-corrected using manual segmentation

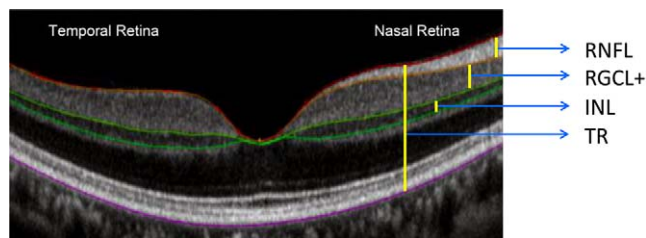


**FIGURE 2.** An fd-OCT scan through the fovea of a healthy control showing the segments measured in the study. The colored lines correspond to the boundaries of different retinal layers identified during the segmentation process. Bar lines indicate different retinal thickness measurements.

via a custom program as described previously,<sup>13,24,25</sup> a technique that has been shown to provide reliable and repeatable results.<sup>26</sup> Hand correction was done by an experienced operator blinded to the patient's diagnosis during the segmentation process. After segmentation, we calculated the following thickness parameters: macular RNFL (mRNFL), RGCL combined with the inner plexiform layer (IPL), and INL. Because the boundary between RGCL and IPL sometimes can be hard to determine, we combined the two layers into one parameter (RGCL+) rather than measure them separately (Fig. 2). For each cube scan, we segmented 128 B-scans and obtained the thickness for each evaluated layer, including 4 separate measurements corresponding to mRNFL, RGCL+, INL, and total retinal (TR) thickness. A pseudo-color thickness map of these layers is shown in Figure 3 for one control, and three eyes with BA of the optic nerve and variable degrees of temporal VF loss.

All acquired macular cube scans were assessed qualitatively for microcystic abnormalities in the INL as well as other abnormalities of the retina or vitreoretinal interface. Microcystic abnormalities were defined as cystic, lacunal areas of hyporeflectivity with clear boundaries, evident on at least two contiguous scans.<sup>20</sup>

### Visual Function Testing

The subjects underwent a complete ophthalmologic examination, including best-corrected monocular visual acuity assessment and SAP. The SAP was conducted with a Humphrey Field

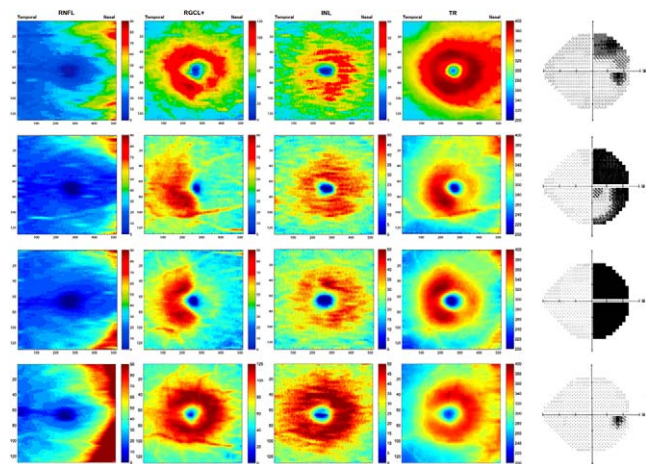


**FIGURE 3.** Pseudocolor thickness map generated from cube scan based on the thickness of the layers evaluated. First, second, and third lines indicate eyes with band atrophy of the optic nerve and different degrees of visual field loss. Fourth line indicates a normal control.

Analyzer (Carl-Zeiss Meditec, Dublin, CA, USA) using the Swedish Interactive Threshold Algorithm (SITA-standard 24-2 program) and a Goldmann size III stimulus on a 31.5-apositlb background. Perimetry was performed on the same day as OCT testing.

The quantification of VF sensitivity loss in patients and controls was based on the global mean defect (MD) and on the analysis of 16 central points of the VF; an area roughly equivalent to the area covered by 3D OCT-1000 raster scanning in the macular area. The values of the total deviation plot of the SAP 24-2 test covering these 16 test points ( $18^\circ \times 18^\circ$ ) were averaged globally to calculate the central mean deviation (CMD) and the deviation of each quadrant (superotemporal, inferotemporal, superonasal, and inferonasal), each one representing the average deviation of four VF test points (Fig. 1). Each number represents the difference, expressed in decibels (dB), between the threshold luminance for that participant and that of a group of age-matched healthy controls. For each calculation, the deviation from normal at each test location was converted from dB to 1/Lambert (1/L) units by dividing the dB value by 10 and unlogging the quotient. This conversion is based upon the assumption that the relationship between structure and function is linear when visual field measures are expressed on a linear scale.<sup>1</sup> Relative sensitivity was calculated globally and for each VF sector in patients and controls, and expressed in dB and 1/L units.

### Data Analysis and Statistics

Macular thickness values of eyes with BA and normal controls were compared using Student's *t*-test. The analysis of the histograms and the Shapiro-Wilk test confirmed that the distributions satisfied the normality assumption. Receiver operating characteristic (ROC) curves were used to describe the ability of OCT parameters to discriminate BA from control eyes. The method of DeLong et al.<sup>27</sup> was used to compare areas under the ROC curves (AUCs).

The association between retinal measurements and VF sensitivity loss was tested using either Spearman's ranked correlation coefficients ( $\rho$ ) for VF values in decibels (dB) or Pearson's correlation coefficients (*r*) for VF values in 1/L units. Subsequently, the relationship between fd-OCT measurements and VF loss expressed in 1/L scale was described with linear regression analysis based on a previously proposed model.<sup>4</sup> The VF data were treated as dependent variables and fd-OCT measurements as independent variables in all regressions. The incidence of microcysts was compared in the two groups using Fisher's exact test. Analysis was performed using SPSS version 19.0 (SPSS, Inc., Chicago, IL, USA). *P* values of less than 0.05 were considered statistically significant. Results of statistical significance were provided after Bonferroni's correction based on the number of comparisons within each analysis.

### RESULTS

We studied 33 eyes with temporal hemianopia and 36 control eyes. The mean age  $\pm$  SD was  $44.0 \pm 12.0$  years (range, 21-66) in BA patients, and  $38.8 \pm 11.7$  years (range, 23-60) in normal subjects ( $P = 0.07$ , Student's *t*-test). The fundoscopic examination revealed signs of BA of the optic disc and peripapillary RNFL in all 33 eyes.

Table 1 and Figure 4 show macular thickness parameters for each quadrant in patients and controls. After Bonferroni's correction ( $\alpha = 0.003$ , 16 comparisons), mRNFL, RGCL+, and TR thickness measurements were significantly smaller ( $P < 0.001$ ) in BA compared to controls in each evaluated quadrant. The largest differences were found in the nasal hemiretina, as

**TABLE 1.** Mean Values ( $\pm$ SD) of Macular Thickness Parameters (in  $\mu\text{m}$ ) in Different Layers and Areas of the Retina, With AUC and Sensitivities at Fixed Specificities

Parameter	Band Atrophy, <i>n</i> = 33	Controls, <i>n</i> = 36	<i>P</i> <sup>*</sup>	AUC (SE)
<b>Superior temporal quadrant</b>				
RNFL	20.4 $\pm$ 2.7	24.4 $\pm$ 2.4	<0.001†	0.89 (0.04)
RGCL+	59.0 $\pm$ 7.7	68.3 $\pm$ 6.4	<0.001†	0.83 (0.05)
INL	32.1 $\pm$ 2.2	30.9 $\pm$ 2.7	0.05	0.63 (0.07)
TR	277.1 $\pm$ 10.2	286.3 $\pm$ 14.2	0.003†	0.68 (0.06)
<b>Inferior temporal quadrant</b>				
RNFL	21.4 $\pm$ 2.4	25.4 $\pm$ 2.8	<0.001†	0.88 (0.04)
RGCL+	61.4 $\pm$ 7.4	70.2 $\pm$ 5.3	<0.001†	0.83 (0.05)
INL	31.7 $\pm$ 2.0	31.0 $\pm$ 2.5	0.23	0.58 (0.07)
TR	276.3 $\pm$ 9.9	285.0 $\pm$ 12.7	0.002†	0.70 (0.06)
<b>Superior nasal quadrant</b>				
RNFL	28.6 $\pm$ 8.0	51.7 $\pm$ 7.7	<0.001†	0.98 (0.01)
RGCL+	50.3 $\pm$ 7.3	70.4 $\pm$ 6.7	<0.001†	0.98 (0.01)
INL	35.5 $\pm$ 3.6	32.2 $\pm$ 2.7	<0.001†	0.77 (0.06)
TR	285.1 $\pm$ 12.1	319.1 $\pm$ 15.5	<0.001†	0.96 (0.02)
<b>Inferior nasal quadrant</b>				
RNFL	33.1 $\pm$ 9.5	55.8 $\pm$ 10.4	<0.001†	0.94 (0.02)
RGCL+	49.18 $\pm$ 6.7	69.7 $\pm$ 5.6	<0.001†	0.99 (0.01)
INL	34.2 $\pm$ 2.8	31.3 $\pm$ 2.8	<0.001†	0.77 (0.06)
TR	282.0 $\pm$ 13.3	314.8 $\pm$ 15.2	<0.001†	0.95 (0.02)

\* Student's *t*-test.  
† Significant values.

shown in Figure 4. The INL thickness measurements, on the other hand, were significantly greater in the superior and inferior nasal quadrants of BA eyes compared to normal controls ( $P < 0.001$ ), while no significant differences were observed between temporal quadrant measurements. The INL microcysts were found in seven eyes with BA in the nasal half of the macula (Fig. 5), but not in any of the control eyes ( $P =$

0.004). The best areas AUCs for distinguishing between BA eyes and controls were those of RGCL+ thickness in the inferior nasal quadrant (0.99) and in the superior nasal quadrant (0.98) and RNFL thickness in the superior nasal quadrant (0.98). No significant difference was observed between AUCs corresponding to TR, RNFL, and RGCL+ measurements in the superior and inferior nasal quadrants. The AUCs corresponding to the RNFL measurements in superotemporal (0.89) and inferotemporal (0.88) quadrants were significantly greater ( $P = 0.002$  and  $0.01$ , respectively) than those corresponding to the TR measurement (0.68 and 0.70). The AUCs from RGCL+ in the superior and inferior temporal quadrants (0.83 for both measurements) also were significantly greater ( $P = 0.002$  and  $0.01$ , respectively) compared to AUCs corresponding to TR in the same quadrants. No significant difference was observed between RNFL and RGCL+ in any quadrant. The AUCs from INL measurements were significantly smaller than those from RNFL or RGCL+ in all quadrants and than those from TR in the nasal quadrants ( $P < 0.01$ ). The AUCs from INL measurements did not differ from those of TR measurements in the superior or inferior temporal quadrants ( $P = 0.65$  and  $0.31$ , respectively). After excluding the seven eyes with microcysts, the mean  $\pm$  SD INL thickness measurement of eyes with BA ( $n = 26$ ) were  $31.64 \pm 1.94$ ,  $31.44 \pm 1.89$ ,  $34.29 \pm 2.17$ , and  $33.69 \pm 2.12 \mu\text{m}$ , in the superior temporal, inferior temporal, superior nasal, and inferior nasal quadrants, respectively. When these values were compared to normal controls, no significant difference was found in measurements from the superior and inferior temporal quadrants ( $P = 0.26$  and  $0.47$ , respectively), while measurements from the superior and inferior nasal quadrants were significantly greater ( $P = 0.002$  and  $0.001$ , respectively).

The mean  $\pm$  SD of global SAP mean deviation of eyes with BA was  $-8.78 \pm 5.19$  dB. Deviation from normal (mean  $\pm$  SD, in dB) based on the 16 central points of the VF in the superior temporal, superior nasal, inferior nasal, and inferior temporal quadrants (four points each) were  $-17.35 \pm 14.54$ ,  $-1.42 \pm$

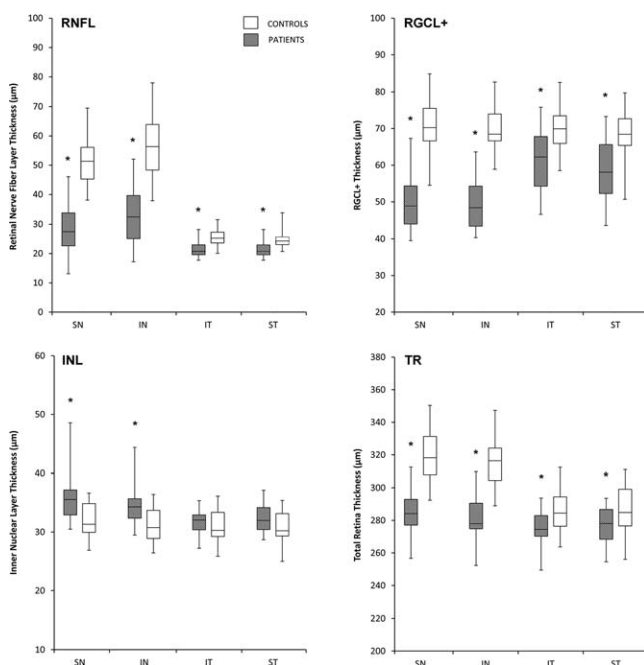


**FIGURE 4.** Box plots illustrating the interquartile range for macular RNFL (upper left), RGCL+ (upper right), INL (lower left), and TR (lower right). \* $P < 0.003$ , compared to controls.

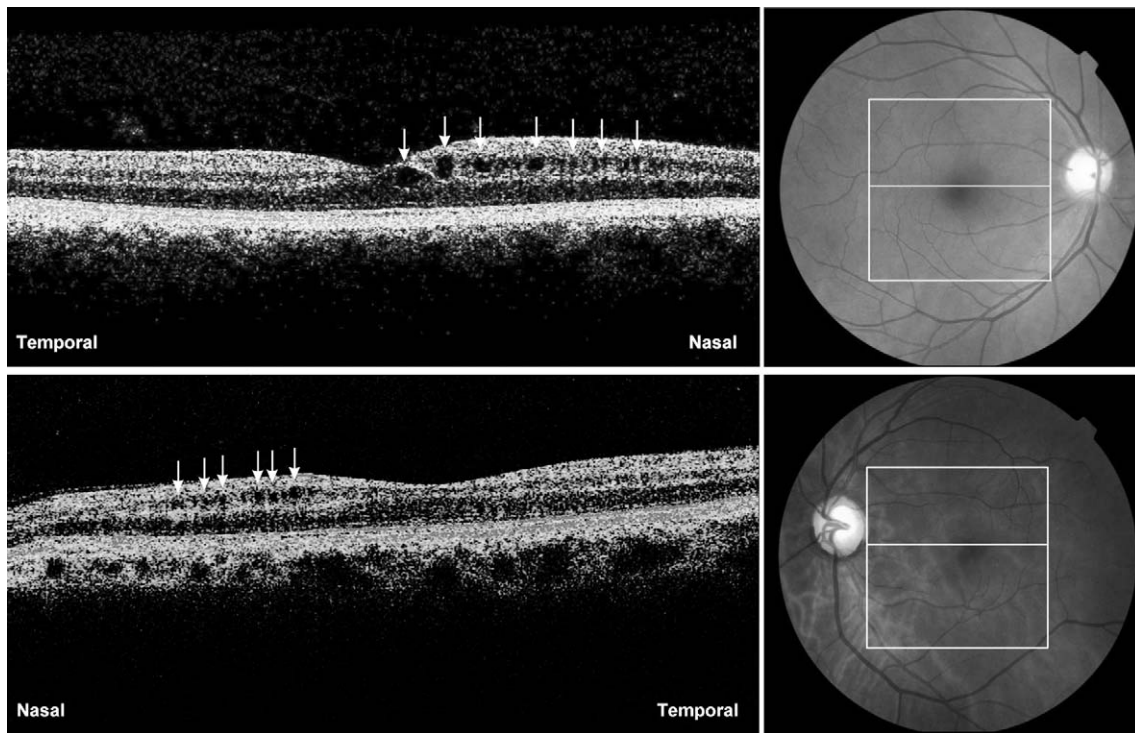


FIGURE 5. The fd-OCT scans through the fovea of a right (above) and left (below) eye of two patients with complete temporal hemianopia and band atrophy of the optic nerve. Retina microcystic (indicated by small arrows) degeneration in the inner nuclear layer are present nasally to the fovea in both eyes.

TABLE 2. Relationship Between fd-OCT Macular Thickness Parameters and VF Sensitivity Parameters Calculated From the 16 Central Points of the VF in SAP

OCT Parameter	Visual Field Parameter (1/L)			
	ST	IT	SN	IN
RNFL thickness				
SN quadrant	0.72*	0.78*	0.15	0.28‡
IN quadrant	0.61*	0.71*	0.22	0.31‡
ST quadrant	0.64*	0.69*	0.30‡	0.41*
IT quadrant	0.52*	0.66*	0.37†	0.46*
RGCL+				
SN quadrant	0.64*	0.81*	0.01	0.13
IN quadrant	0.66*	0.77*	0.02	0.11
ST quadrant	0.44*	0.69*	0.15	0.26‡
IT quadrant	0.48*	0.69*	0.29‡	0.38†
INL				
SN quadrant	-0.54*	-0.53*	-0.24	-0.23
IN quadrant	-0.52*	-0.48*	-0.21	-0.22
ST quadrant	-0.39†	-0.34†	-0.29‡	-0.27‡
IT quadrant	-0.23	-0.20	-0.25	-0.22
TR				
SN quadrant	0.51*	0.67*	-0.02	0.12
IN quadrant	0.49*	0.64*	0.08	0.16
ST quadrant	0.11	0.35†	-0.04	0.08
IT quadrant	0.15	0.37†	0.11	0.17

Pearson correlation coefficient.  
 \*  $P < 0.001$ .  
 †  $P < 0.01$ .  
 ‡  $P < 0.05$ .

2.44,  $-15.60 \pm 13.87$ , and  $-1.54 \pm 1.82$ , respectively. Table 2 shows the correlations between individual inner retinal layer thickness and total retinal thickness, along with the severity of VF loss based on the 16 central points of the VF (in 1/L units). Statistically significant correlations were found for most parameters, particularly between nasal quadrant macular thickness and temporal VF parameters. Correlations with VF loss were positive for mRNFL, RGCL+, and TR measurements, and negative for INL measurements. The strongest correlations were found between the superonasal quadrant RGCL+ thickness measurement and the inferotemporal central VF quadrant (0.81,  $P < 0.001$ ), between superonasal quadrant mRNFL thickness and the inferotemporal central VF quadrant (0.78,  $P < 0.001$ ), and between the inferonasal quadrant RGCL+ thickness and the inferotemporal central VF quadrant (0.77,  $P < 0.001$ , Table 2).

Figure 6 shows the results from the linear regression analysis of the best-performing macular thickness measurements (mRNFL, RGCL+, INL, and TR) and VF loss (in 1/L units). For the mRNFL thickness measurements, the largest sectoral  $R^2$  was observed between inferotemporal VF loss and superonasal mRNFL thickness ( $R^2 = 0.61$ ,  $P < 0.001$ ), followed by superotemporal VF loss and superonasal mRNFL thickness ( $R^2 = 0.52$ ,  $P < 0.001$ ). As for the RGCL+, the greatest  $R^2$  were observed between inferotemporal VF loss and superonasal ( $R^2 = 0.66\%$ ,  $P < 0.001$ ) or inferonasal ( $R^2 = 0.59$ ,  $P < 0.001$ ) macular thickness. The greatest negative sectoral  $R^2$  for INL were observed between superotemporal VF loss and superonasal thickness ( $R^2 = 0.29$ ,  $P < 0.001$ ), and between superotemporal VF loss and inferonasal thickness ( $R^2 = 0.28$ ,  $P < 0.001$ ). With regard to TR thickness, the greatest  $R^2$  were observed between inferotemporal VF loss and superonasal ( $R^2 = 0.45$ ,  $P < 0.001$ ) or inferonasal ( $R^2 = 0.41$ ,  $P < 0.001$ ) quadrant macular thickness.

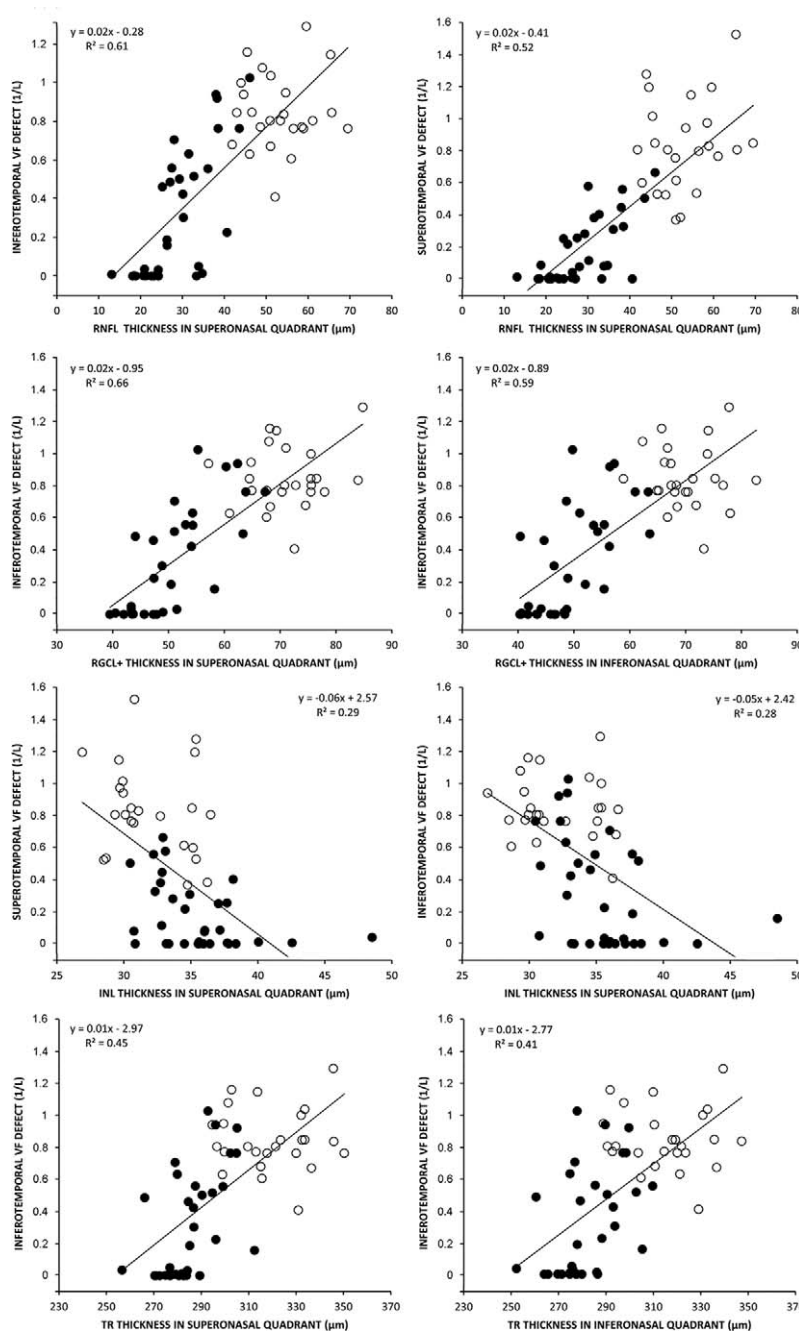


FIGURE 6. Scatterplots of the best performing macular thickness (*upper row*) or RNFL thickness (*lower row*) plotted against the visual field sensitivity loss parameter expressed in the antilog (1/L) scale.

## DISCUSSION

The ability of OCT-measured peripapillary RNFL and TR thickness to quantify axonal loss in chiasmal compressive lesions and discriminate such eyes from controls has been documented in several studies.<sup>8,10,28-30</sup> Previous studies also have shown that macular and peripapillary RNFL OCT measurements correlate with VF loss and possibly could be used for estimating the chances of VF recovery after treatment of patients with chiasmal compression.<sup>28,31,32</sup> Such OCT findings may be particularly useful in patients with suspected or known chiasmal lesions who are not capable of performing reliable VF measurements. While most such studies have investigated the diagnostic ability and structure-function

relationship of peripapillary RNFL thickness measurements, TR macular thickness measurements also have been shown to be useful,<sup>8,9,32</sup> with comparable results for the two sets of measurements.<sup>8</sup>

More recently, the introduction of fd-OCT, which produces images of higher resolution than time-domain OCT, has allowed the segmentation of different layers of the retina in the macular area, including mRNFL, RGCL, and INL. Measuring specific retinal layers makes it possible to obtain stronger associations between macular measurements and functional visual loss. In fact, previous studies have documented improved performance of RGC thickness measurements compared to full-thickness macular measurements in glaucoma.<sup>15</sup> However, only one study has evaluated segmented macular thickness parameters

in patients with chiasmal compression. Ohkubo et al.<sup>33</sup> measured macular and peripapillary RNFL thickness parameters in 12 patients with chiasmal compression from pituitary tumors. The authors found that average macular RGC complex thickness measurements obtained with an automated segmentation protocol were significantly reduced in affected patients compared to controls. Macular RGC complex thickness parameters were correlated significantly with VF defects, but the correlation coefficient of the best-performing parameter (0.41) was not better than the corresponding value for the best-performing peripapillary RNFL thickness parameter (0.56). However, in that study macular RGC measurements were estimated only as average values for the macular area, corresponding to 12 central points in the VF, 10 of which in the nasal field and only two in the temporal (affected) field. Thus, although the authors did, in fact, evaluate corresponding RGC and VF areas, the fact that the OCT scanner provided RGC complex values in a predetermined area only prevented the authors from optimizing the structure-function evaluation.<sup>33</sup>

When performing structure-function relationship analysis between retinal structures and VF defects, it is important to evaluate measurements of specific VF areas with corresponding OCT measurements, taking into consideration the anatomy of the distribution of RGCs and RNFL. In studies using peripapillary RNFL thickness measurements and VF data, a commonly used pattern is the distribution of the fibers around the disc with a corresponding VF map, as defined by Garway-Heath et al.<sup>34</sup> When using this pattern, six areas around the optic disc are correlated with six corresponding areas of the VF, most of which encompass areas of the nasal and the temporal hemiretinas; therefore, not respecting the vertical meridian. On the other hand, for macular thickness measurements, the correspondence with VF areas in patients with chiasmal and retrochiasmal lesions is a more direct one. For example, superior VF defects can be correlated with inferior macular thickness measurements, while temporal VF defects can be correlated with nasal macular thickness measurements.<sup>8</sup> However, most OCT scanners provide macular measurements as global average values or as circular measurements, usually according to the EDTRS map, and, thus, do not respect the vertical meridian. Macular thickness measurements, including the temporal and nasal retina, can be difficult to correlate with VF defects which respect the vertical meridian. In the current study, we were able to analyze retinal thickness measurements divided in four quadrants in patients with temporal VF defects from chiasmal compression, and thereby obtain a stronger structure-function/VF loss correlation. Our results show that the segmentation of macular structures improved diagnostic ability when mRNFL and RGCL+ measurements were compared to TR thickness measurements (Table 1). Improvement in discrimination ability was observed when evaluating the less affected temporal retina of the patients with chiasmal compression. In the severely affected nasal quadrants, TR thickness and isolated segmented macular mRNFL and RGCL+ thickness measurements displayed similar discrimination ability and similar AUCs, but in the least affected superior and inferior temporal quadrant, discrimination ability was better for mRNFL and RGCL+ measurements than for TR thickness measurements. Therefore, our results suggested that the discrimination ability of OCT measurements in eyes with BA of the optic nerve versus healthy controls is greater for segmented mRNFL and RGCL+ macular layers than for TR thickness measurements (Table 1). These findings are in agreement with other studies that also have shown improved performance of segmented macular RGCL+ measurements in glaucoma,<sup>35,36</sup> and MS patients.<sup>37</sup>

In the present study, we documented that mRNFL and RGCL+ thicknesses estimated in different quadrants of the

macula were reduced significantly in patients compared to controls. The mRNFL and RGCL+ measurements were reduced significantly in the nasal retinal quadrants as well as in the temporal retinal quadrants. The observation of reduced thickness of the temporal retinal measurements in this group of eyes has been reported previously<sup>8,10</sup> and probably is due to the fact that in many patients with chiasmal compression the uncrossed fibers from the temporal hemiretina have been damaged before chiasmal decompression. If the OCT is more sensitive than SAP in the assessment of RGC and mRNFL thickness, at least in some patients, then OCT parameters may be affected even when there is a normal nasal VF examination. In fact, since our patients were treated for previous chiasmal compression, the nasal VF (temporal hemiretina) may have been affected by the compression of the uncrossed temporal fibers at the optic chiasm.

In addition, the INL thickness was increased significantly in BA patients versus controls in the nasal hemiretina. Furthermore, microcystic abnormalities in the INL (Fig. 5) were observed in a significant number of patients with BA of the optic nerve, but not in controls. In a previous study evaluating patients with NMO, INL thickness was greater in patients than in normals.<sup>12</sup> In that study, we speculated that the increase might be the result of edema in the INL somehow related to the existence of aquaporin 4 protein, which is the target of antibodies in NMO patients.<sup>12</sup> Likewise, microcystic abnormalities in the INL of patients with MS were described recently and initially attributed to retinal edema in such patients.<sup>16</sup> However, subsequent studies on demyelinating diseases,<sup>19,20</sup> hereditary<sup>38</sup> and compressive optic pathway diseases,<sup>22</sup> and glaucoma suggest that microcystic degeneration in the INL is similar to the cystic cavitations observed histopathologically in the INL of enucleated human eyes with optic nerve lesions.<sup>22,39</sup> On the other hand, Barboni et al.<sup>38</sup> proposed that trans-synaptic degeneration alone could not explain the phenomena and that vitreous traction should be a likely additional factor for the occurrence of retinal microcysts. Our results are unique in finding microcystic retinal degeneration in a large percentage of eyes (7 out of 33) with BA of the optic nerve. Vitreous traction seems an unlikely pathogenic factor, as the microcysts were restricted to the nasal side of the macula (Fig. 5), corresponding to the more strongly affected temporal VF. Interestingly, our data also showed that, while BA eyes and controls display similar INL thickness in the temporal hemiretina, the INL clearly is thicker in the nasal hemiretina, which corresponds to the more severe axonal loss in that area.

When we excluded the seven eyes with microcysts, INL still was thicker in the nasal retina of BA eyes compared to controls. These data strongly suggested that increased INL thickness is, in fact, part of a reactive process secondary to axonal degeneration and may precede the development of microcystic degeneration. However, further studies preferably using high-resolution raster scanning of the macula are needed to evaluate the actual incidence of microcysts in eyes with BA of the optic nerve and identify the pathogenic mechanisms involved.

In the current study, we also investigated the usefulness of segmenting retinal layers and obtaining thickness measurements in quadrants for improving performance in the assessment of structure-function relationships in patients with temporal field defects. Our findings clearly indicated improved performance for segmented retinal layers compared to TR thickness measurements of the retina for studies of structure-function relationship. While the greatest correlation coefficients for TR thickness measurements was 0.72, the corresponding figures for mRNFL and RGCL+ layers were 0.78 and 0.81, respectively. Analysis of the data in Table 2 and the results of linear regression analysis also yielded stronger correlations

for segmented mRNFL and RGCL+ measurements than for TR thickness measurements (Fig. 5). The correlation coefficients of the segmented mRNFL and RGCL+ measurements also were superior to those of the best-performing peripapillary RNFL thickness measurements (0.60) in a previous study based on a similar group of patients.<sup>8</sup>

In conclusion, the current study showed that axonal degeneration in BA eyes leads to significant mRNFL and RGCL+ thinning and INL thickening compared to controls and that measuring segmented layers of the retina divided in quadrants provides adequate data for differentiating such eyes from normal controls. It also showed that mRNFL and RGCL+ measurements correlate strongly with VF loss and are more useful than TR thickness measurements when assessing the structure-function relationship. Segmented macular thickness measurements may be useful for quantifying neuronal loss in patients with chiasmal compression.

### Acknowledgments

Supported by grants from Fundação de Amparo a Pesquisa do Estado de São Paulo FAPESP (No. 2009/50174-0), São Paulo, Brazil, and from Conselho Nacional de Desenvolvimento Científico e Tecnológico, CNPq (No. 306487/2011-0), Brasília, Brazil.

Disclosure: **M.L.R. Monteiro**, None; **K. Hokazono**, None; **D.B. Fernandes**, None; **L.V.F. Costa-Cunha**, None; **R.M. Sousa**, None; **A.S. Raza**, None; **D.L. Wang**, None; **D.C. Hood**, None

### References

- Hood DC, Kardon RH. A framework for comparing structural and functional measures of glaucomatous damage. *Prog Retin Eye Res.* 2007;26:688-710.
- Monteiro ML, Fernandes DB, Apostolos-Pereira SL, Callegaro D. Quantification of retinal neural loss in patients with neuromyelitis optica and multiple sclerosis with or without optic neuritis using Fourier-domain optical coherence tomography. *Invest Ophthalmol Vis Sci.* 2012;53:3959-3966.
- Barboni P, Savini G, Parisi V, et al. Retinal nerve fiber layer thickness in dominant optic atrophy measurements by optical coherence tomography and correlation with age. *Ophthalmology.* 2011;118:2076-2080.
- Hood DC, Anderson S, Rouleau J, et al. Retinal nerve fiber structure versus visual field function in patients with ischemic optic neuropathy. A test of a linear model. *Ophthalmology.* 2008;115:904-910.
- Unsold R, Hoyt WF. Band atrophy of the optic nerve. The histology of temporal hemianopsia. *Arch Ophthalmol.* 1980;98:1637-1638.
- Danesh-Meyer HV, Papchenko T, Savino PJ, Law A, Evans J, Gamble GD. In vivo retinal nerve fiber layer thickness measured by optical coherence tomography predicts visual recovery after surgery for parachiasmal tumors. *Invest Ophthalmol Vis Sci.* 2008;49:1879-1885.
- Monteiro ML, Moura FC, Medeiros FA. Diagnostic ability of optical coherence tomography with a normative database to detect band atrophy of the optic nerve. *Am J Ophthalmol.* 2007;143:896-899.
- Monteiro ML, Costa-Cunha LV, Cunha LP, Malta RF. Correlation between macular and retinal nerve fibre layer Fourier-domain OCT measurements and visual field loss in chiasmal compression. *Eye (Lond).* 2010;24:1382-1390.
- Moura FC, Medeiros FA, Monteiro ML. Evaluation of macular thickness measurements for detection of band atrophy of the optic nerve using optical coherence tomography. *Ophthalmology.* 2007;114:175-181.
- Costa-Cunha LV, Cunha LP, Malta RF, Monteiro ML. Comparison of Fourier-domain and time-domain optical coherence tomography in the detection of band atrophy of the optic nerve. *Am J Ophthalmol.* 2009;147:56-63.
- Saidha S, Syc SB, Durbin MK, et al. Visual dysfunction in multiple sclerosis correlates better with optical coherence tomography derived estimates of macular ganglion cell layer thickness than peripapillary retinal nerve fiber layer thickness. *Mult Scler.* 2011;17:1449-1463.
- Fernandes DB, Raza AS, Nogueira RG, et al. Evaluation of inner retinal layers in patients with multiple sclerosis or neuromyelitis optica using optical coherence tomography. *Ophthalmology.* 2013;120:387-394.
- Wang M, Hood DC, Cho JS, et al. Measurement of local retinal ganglion cell layer thickness in patients with glaucoma using frequency-domain optical coherence tomography. *Arch Ophthalmol.* 2009;127:875-881.
- Syc SB, Saidha S, Newsome SD, et al. Optical coherence tomography segmentation reveals ganglion cell layer pathology after optic neuritis. *Brain.* 2012;135:521-533.
- Tan O, Chopra V, Lu AT, et al. Detection of macular ganglion cell loss in glaucoma by Fourier-domain optical coherence tomography. *Ophthalmology.* 2009;116:2305-2314, e2301-e2302.
- Gelfand JM, Nolan R, Schwartz DM, Graves J, Green AJ. Microcystic macular oedema in multiple sclerosis is associated with disease severity. *Brain.* 2012;135:1786-1793.
- Saidha S, Sotirchos ES, Ibrahim MA, et al. Microcystic macular oedema, thickness of the inner nuclear layer of the retina, and disease characteristics in multiple sclerosis: a retrospective study. *Lancet Neurol.* 2012;11:963-972.
- Balk LJ, Killestein J, Polman CH, Uitdehaag BM, Petzold A. Microcystic macular oedema confirmed, but not specific for multiple sclerosis. *Brain.* 2012;135:e226, author reply e227.
- Gelfand JM, Cree BA, Nolan R, Arnov S, Green AJ. Microcystic inner nuclear layer abnormalities and neuromyelitis optica. *JAMA Neurol.* 2013;70:629-633.
- Sotirchos ES, Saidha S, Byraiah G, et al. In vivo identification of morphologic retinal abnormalities in neuromyelitis optica. *Neurology.* 2013;80:1406-1414.
- Wolff B, Basdekidou C, Vasseur V, Mauget-Faysse M, Sahel JA, Vignal C. Retinal inner nuclear layer microcystic changes in optic nerve atrophy: a novel spectral-domain OCT finding. *Retina.* 2013;33:2133-2138.
- Abegg M, Zinkernagel M, Wolf S. Microcystic macular degeneration from optic neuropathy. *Brain.* 2012;135:e225.
- Yang Q, Reisman CA, Wang Z, et al. Automated layer segmentation of macular OCT images using dual-scale gradient information. *Opt Express.* 2010;18:21293-21307.
- Raza AS, Cho J, de Moraes CG, et al. Retinal ganglion cell layer thickness and local visual field sensitivity in glaucoma. *Arch Ophthalmol.* 2011;129:1529-1536.
- Hood DC, Lin CE, Lazow MA, Locke KG, Zhang X, Birch DG. Thickness of receptor and post-receptor retinal layers in patients with retinitis pigmentosa measured with frequency-domain optical coherence tomography. *Invest Ophthalmol Vis Sci.* 2009;50:2328-2336.
- Hood DC, Cho J, Raza AS, Dale EA, Wang M. Reliability of a computer-aided manual procedure for segmenting optical coherence tomography scans. *Optom Vis Sci.* 2011;88:113-123.
- DeLong ER, DeLong DM, Clarke-Pearson DL. Comparing the areas under two or more correlated receiver operating characteristic curves: a nonparametric approach. *Biometrics.* 1988;44:837-845.
- Danesh-Meyer HV, Carroll SC, Foroozan R, et al. Relationship between retinal nerve fiber layer and visual field sensitivity as measured by optical coherence tomography in chiasmal compression. *Invest Ophthalmol Vis Sci.* 2006;47:4827-4835.

29. Monteiro ML, Leal BC, Rosa AA, Bronstein MD. Optical coherence tomography analysis of axonal loss in band atrophy of the optic nerve. *Br J Ophthalmol*. 2004;88:896-899.
30. Kanamori A, Nakamura M, Matsui N, et al. Optical coherence tomography detects characteristic retinal nerve fiber layer thickness corresponding to band atrophy of the optic discs. *Ophthalmology*. 2004;111:2278-2283.
31. Jacob M, Raverot G, Jouanneau E, et al. Predicting visual outcome after treatment of pituitary adenomas with optical coherence tomography. *Am J Ophthalmol*. 2009;147:64-70.
32. Monteiro ML, Cunha LP, Costa-Cunha LV, Maia OO Jr, Oyamada MK. Relationship between optical coherence tomography, pattern electroretinogram and automated perimetry in eyes with temporal hemianopia from chiasmal compression. *Invest Ophthalmol Vis Sci*. 2009;50:3535-3541.
33. Ohkubo S, Higashide T, Takeda H, Murotani E, Hayashi Y, Sugiyama K. Relationship between macular ganglion cell complex parameters and visual field parameters after tumor resection in chiasmal compression. *Jpn J Ophthalmol*. 2012;56:68-75.
34. Garway-Heath DF, Poinosawmy D, Fitzke FW, Hitchings RA. Mapping the visual field to the optic disc in normal tension glaucoma eyes. *Ophthalmology*. 2000;107:1809-1815.
35. Mwanza JC, Durbin MK, Budenz DL, et al. Glaucoma diagnostic accuracy of ganglion cell-inner plexiform layer thickness: comparison with nerve fiber layer and optic nerve head. *Ophthalmology*. 2012;119:1151-1158.
36. Nakano N, Hangai M, Nakanishi H, et al. Macular ganglion cell layer imaging in preperimetric glaucoma with speckle noise-reduced spectral domain optical coherence tomography. *Ophthalmology*. 2011;118:2414-2426.
37. Walter SD, Ishikawa H, Galetta KM, et al. Ganglion cell loss in relation to visual disability in multiple sclerosis. *Ophthalmology*. 2012;119:1250-1257.
38. Barboni P, Carelli V, Savini G, Carbonelli M, La Morgia C, Sadun AA. Microcystic macular degeneration from optic neuropathy: not inflammatory, not trans-synaptic degeneration. *Brain*. 2013;136:e239.
39. Gills JP Jr, Wadsworth JA. Degeneration of the inner nuclear layer of the retina following lesions of the optic nerve. *Trans Am Ophthalmol Soc*. 1966;64:66-88.
40. Hood DC, Raza AS, de Moraes CG, Liebmann JM, Ritch R. Glaucomatous damage of the macula. *Prog Retin Eye Res*. 2013;32:1-21.